Acta Cryst E CRYSTALLOGRAPHIC COMMUNICATIONS

ISSN 2056-9890

Crystal structures of two dis-symmetric di-Schiff base compounds: 2-({(*E*)-2-[(*E*)-2,6-dichlorobenzylidene]hydrazin-1-ylidene}methyl)-6-methoxyphenol and 4-bromo-2-({(*E*)-2-[(*E*)-2,6-dichlorobenzylidene]hydrazin-1-ylidene}methyl)phenol

Received 12 May 2020
Accepted 13 May 2020

Edited by W. T. A. Harrison, University of Aberdeen, Scotland

‡ Additional correspondence author, e-mail: drmks2000hotmail.com.

Keywords: crystal structure; Schiff base; Hirshfeld surface analysis; computational chemistry.

CCDC references: 2003762; 2003761

Supporting information: this article has supporting information at journals.iucr.org/e

Rohit B. Manawar,[a] Chandankumar T. Pashavan,[a] Manish K. Shah,[a]‡ Mukesh M. Jotani[b] and Edward R. T. Tiekink[c]*

[a]Chemical Research Laboratory, Department of Chemistry Saurashtra University, Rajkot - 360005, Gujarat, India, [b]Department of Physics, Bhavan's Sheth R. A. College of Science, Ahmedabad, Gujarat 380001, India, and [c]Research Centre for Crystalline Materials, School of Science and Technology, Sunway University, 47500 Bandar Sunway, Selangor Darul Ehsan, Malaysia. *Correspondence e-mail: edwardt@sunway.edu.my

Each of the title dis-symmetric di-Schiff base compounds, $C_{15}H_{12}Cl_2N_2O_2$ (I) and $C_{14}H_9BrCl_2N_2O$ (II), features a central azo-N—N bond connecting two imine groups, each with an *E*-configuration. One imine bond in each molecule connects to a 2,6-dichlorobenzene substituent while the other links a 2-hydroxyl-3-methoxy-substituted benzene ring in (I) or a 2-hydroxyl-4-bromo benzene ring in (II). Each molecule features an intramolecular hydroxyl-O—H···N(imine) hydrogen bond. The C—N—N—C torsion angles of −151.0 (3)° for (I) and 177.8 (6)° (II) indicates a significant twist in the former. The common feature of the molecular packing is the formation of supramolecular chains. In (I), the linear chains are aligned along the *a*-axis direction and the molecules are linked by methoxy-C—H···O(methoxy) and chlorobenzene-C—Cl···π(chlorobenzene) interactions. The chain in (II) is also aligned along the *a* axis but, has a zigzag topology and is sustained by Br···O [3.132 (4) Å] secondary bonding interactions. In each crystal, the chains pack without directional interactions between them. The non-covalent interactions are delineated in the study of the calculated Hirshfeld surfaces. Dispersion forces make the most significant contributions to the identified intermolecular interactions in each of (I) and (II).

1. Chemical context

Schiff base molecules, known for their ease of formation, can be deprotonated to form a prominent class of multidentate ligands for a full range of metal ions leading to a rich coordination chemistry (Vigato & Tamburini, 2004; Clarke & Storr, 2014). The broad range of biological activities exhibited by Schiff base molecules such as anti-bacterial, anti-viral, anti-fungal, anti-malarial, anti-inflammatory, *etc*. (Naeimi *et al.*, 2013; Mukherjee *et al.*, 2013) is a key motivation for studies in this area. Indeed, this is the motivation for the preparation of dis-symmetric di-Schiff base molecules (Liu *et al.*, 2018) related to the title compounds and their transition-metal complexes (Manawar *et al.*, 2019*a*), complemented by crystallographic studies (Manawar *et al.*, 2019*b*, 2020). In a continuation of these structural studies, the crystal and molecular structures of methoxy- (I) and bromine-substituted (II) analogues of an earlier published dis-symmetric di-Schiff base

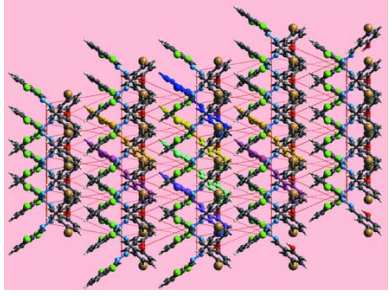

(Manawar *et al.*, 2019*b*) are described herein, together with the detailed analysis of the molecular packing by Hirshfeld surface analysis and computation of energy frameworks.

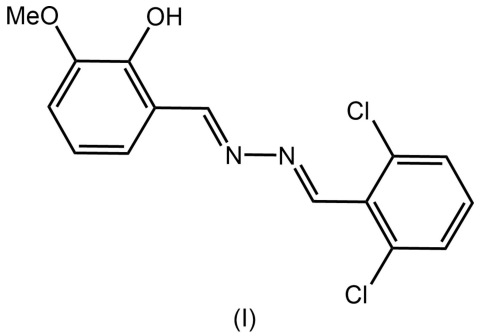

(I)

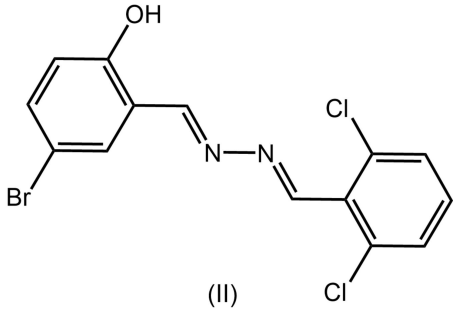

(II)

2. Structural commentary

The molecular structures of (I) and (II) are shown in Fig. 1. The common feature of each molecule is the presence of two imine bonds connected by a azo-N—N bond, Table 1. At one end of each molecule is a 2,6-dichlorobenzene substituent. In (I), the molecule is terminated by a 2-hydroxyl-3-methoxy-substituted benzene ring and in (II), the terminal group is a 2-hydroxyl-4-bromo benzene ring. The configuration about each of the imine bonds is *E*. Each molecule features an intramolecular hydroxyl-O—H···N(imine) hydrogen bond with geometric details listed in Tables 2 and 3, respectively. As might be expected and judged from the data in Table 1, there is a close similarity in comparable geometric parameters characterizing molecules (I) and (II) with salient bond lengths being equal within experimental error. The most significant difference in bond angles is seen in the *ca* 3° wider C9—C8—N2 angle in (II) *cf.* (I). There is an apparent difference in conformation in the central region of the molecules as seen in the *ca* 25° difference in the C7—N1—N2—C8 torsion angles indicating a discernible kink in (I). The central C_2N_2 chromophore in (I) exhibits distortions from co-planarity as the r.m.s. deviation of the fitted atoms is 0.1459 Å with maximum deviations to either side of the plane being 0.155 (17) Å for the N2 atom and 0.149 (14) Å for C8. By contrast, the r.m.s. deviation for the central atoms in (II) is 0.0112 Å. Further differences are noted in dihedral angles between the central plane and pendant benzene rings, and between the benzene rings, Table 1, with the maximum difference occurring for the (C7,N1,N2,C8)/(C9–C14) dihedral angles of 23.1 (4) and 1.5 (6)° for (I) and (II), respectively.

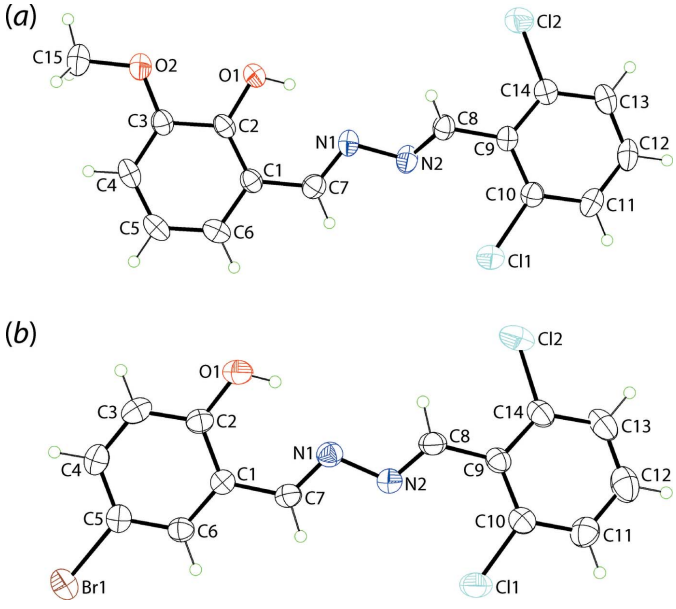

Figure 1
The molecular structures of (*a*) (I) and (*b*) (II), showing the atom-labelling schemes and displacement ellipsoids at the 35% probability level.

Table 1
Selected geometric parameters (Å, °) in (I) and (II).

Parameter	(I)	(II)
N1—N2	1.409 (3)	1.417 (7)
C7—N1	1.283 (3)	1.276 (7)
C8—N2	1.256 (4)	1.234 (7)
N2—N1—C7	112.4 (2)	110.9 (5)
N1—N2—C8	114.2 (2)	114.9 (5)
C1—C7—N1	122.6 (3)	123.1 (6)
C9—C8—N2	121.1 (3)	124.5 (6)
C7—N1—N2—C8	−151.0 (3)	177.8 (6)
C1—C7—N1—N2	−178.8 (2)	−178.9 (5)
C9—C8—N2—N1	179.9 (2)	−179.2 (6)
(C7,N1,N2,C8)/(C1–C6)	20.9 (4)	15.6 (5)
(C7,N1,N2,C8)/(C9–C14)	23.1 (4)	1.5 (6)
(C1–C6)/(C9–C14)	2.41 (17)	15.5 (3)

Table 2
Hydrogen-bond geometry (Å, °) for (I).

*Cg*1 is the centroid of the (C9–14) ring.

D—H···*A*	*D*—H	H···*A*	*D*···*A*	*D*—H···*A*
O1—H1*O*···N1	0.83 (3)	1.91 (3)	2.657 (3)	149 (3)
C15—H15*B*···O2^{i}	0.96	2.58	3.439 (4)	149
C14—Cl2···*Cg*1^{ii}	1.74 (1)	3.70 (1)	3.765 (3)	79 (1)

Symmetry codes: (i) $x-\frac{1}{2}, -y+\frac{5}{2}, -z$; (ii) $x-1, y, z$.

Table 3
Hydrogen-bond geometry (Å, °) for (II).

D—H···*A*	*D*—H	H···*A*	*D*···*A*	*D*—H···*A*
O1—H1*O*···N1	0.83 (6)	1.96 (6)	2.655 (8)	141 (7)

3. Supramolecular features

The two prominent directional interactions in the molecular packing of (I) are of the type C—H···O and C—Cl···π, Table 2. Thus, methoxy-C—H···O(methoxy) and chlorobenzene-C—Cl···π(chlorobenzene) contacts serve to link molecules into supramolecular chain aligned along the *a*-axis direction, Fig. 2(*a*). The linear chains thus formed assemble in the crystal without directional contacts between them, Fig. 2(*b*).

Supramolecular chains along the *a* axis are also noted in the packing of (II), Fig. 3(*a*). In this instance, the contacts between molecules are of the type Br···O, *i.e.* the Br1···O1 separation is 3.132 (4) Å for symmetry operation $\frac{1}{2}+x, 3-y, z$. With the first such interaction in a crystal being reported in 1954, *i.e.* in the crystal of $Br_2{\cdot}O(CH_2CH_2)_2O$ (Hassel & Hvoslef, 1954), these well-described secondary bonding interactions (Alcock, 1972), are termed halogen-bonding interactions in the current parlance (Tiekink, 2017). In (II), the Br···O interactions assemble molecules into zigzag chains as these are propagated by glide symmetry. Globally, the supramolecular chains stack along the *b* axis to form layers and the layers stack along the *c* axis in an ...*ABAB*... fashion, Fig. 3(*b*), but there are no directional interactions between the chains.

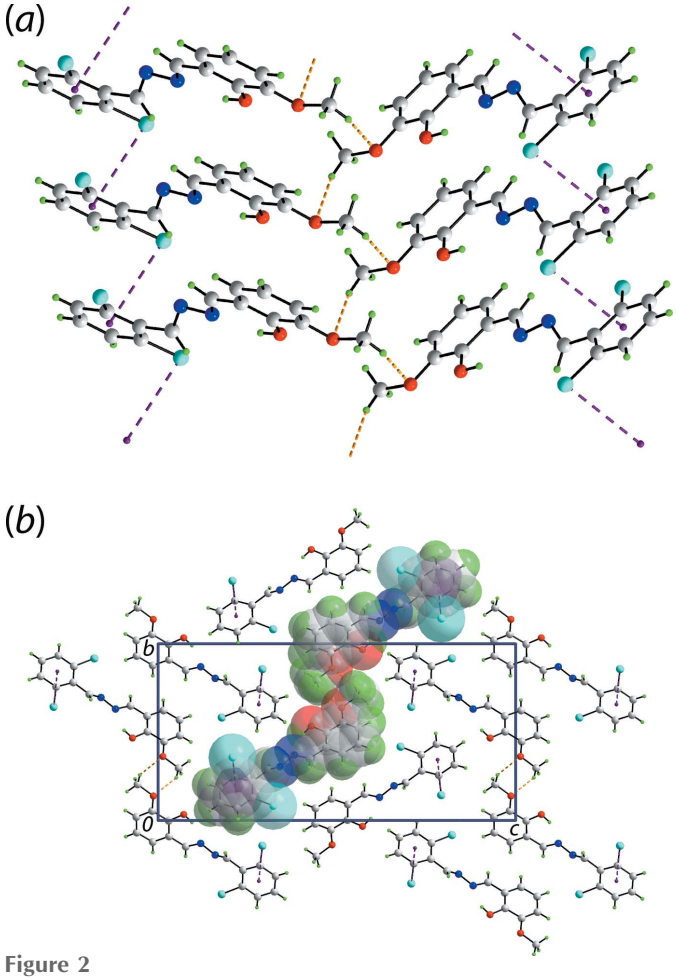

Figure 2
Molecular packing in the crystal of (I): (*a*) supramolecular chain sustained by methoxy-C—H···O(methoxy) and chlorobenzene-C—Cl···π(chlorobenzene) interactions shown as orange and purple dashed lines, respectively and (*b*) a view of the unit-cell contents in projection down the *a* axis with one chain highlighted in space-filling mode.

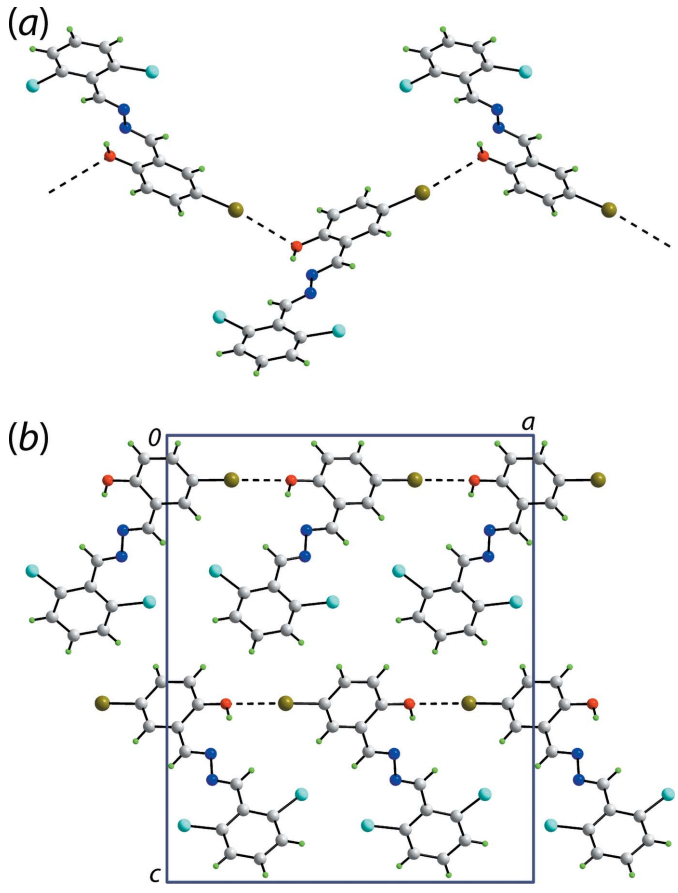

Figure 3
Molecular packing in the crystal of (II): (*a*) supramolecular, zigzag chain sustained by Br···O secondary bonding interactions shown as black dashed lines and (*b*) a view of the unit-cell contents in projection down the *b* axis.

4. Hirshfeld surface analysis

The Hirshfeld surfaces for (I) and (II) were calculated employing the *Crystal Explorer 17* program (Turner *et al.*, 2017) following recently published protocols (Tan *et al.*, 2019). The results describe the influence of non-bonded interactions upon the molecular packing in the crystals of (I) and (II), especially in the absence of directional interactions between the chains.

On the Hirshfeld surfaces mapped over d_{norm}, the presence of the bright-red spots near the methoxy-O2 and H15*B* atoms for (I) in Fig. 4(*a*),(*b*) and those near the Br1 and hydroxyl-O1 atoms in Fig. 5(*a*) for (II), are indicative of dominant intermolecular C—H···O and Br···O contacts in their respective crystal structures. The faint-red spots viewed near the imine-N2 and H8 atoms for (I), and near the Cl2 and H7 atoms for (II) in Fig. 4(*a*),(*b*) and 5(*b*), respectively, indicate the influence of short interatomic contacts (Table 4) on their molecular packing. The Hirshfeld surfaces mapped over the calculated

Table 4
Summary of short interatomic contacts (Å) for (I) and (II)[a].

Contact	Distance	Symmetry operation
(I)		
H12···O1	2.59	$-x, \frac{1}{2}+y, \frac{1}{2}-z$
H8···N2	2.58	$-1+x, y, z$
H13···H15*A*	2.30	$\frac{1}{2}+x, 2-y, \frac{1}{2}+z$
(II)		
Br1···O1	3.132 (4)	$\frac{1}{2}+x, 3-y, z$
Cl2···H7	2.69	$-\frac{1}{2}+x, 1-y, z$

Notes: (*a*) The interatomic distances are calculated in *Crystal Explorer* (Turner *et al.*, 2017) whereby the *X*—H bond lengths are adjusted to their neutron values.

electrostatic potential for (I) and (II) showing contributions from different intermolecular interactions are illustrated through blue and red regions corresponding to positive and negative electrostatic potential in Fig. 6. For (I), the presence of a short C—Cl2···π(C9–C14) contact, Table 2, is illustrated through a blue bump and a orange concave region in the Hirshfeld surface mapped with the shape-index property in Fig. 4(*c*).

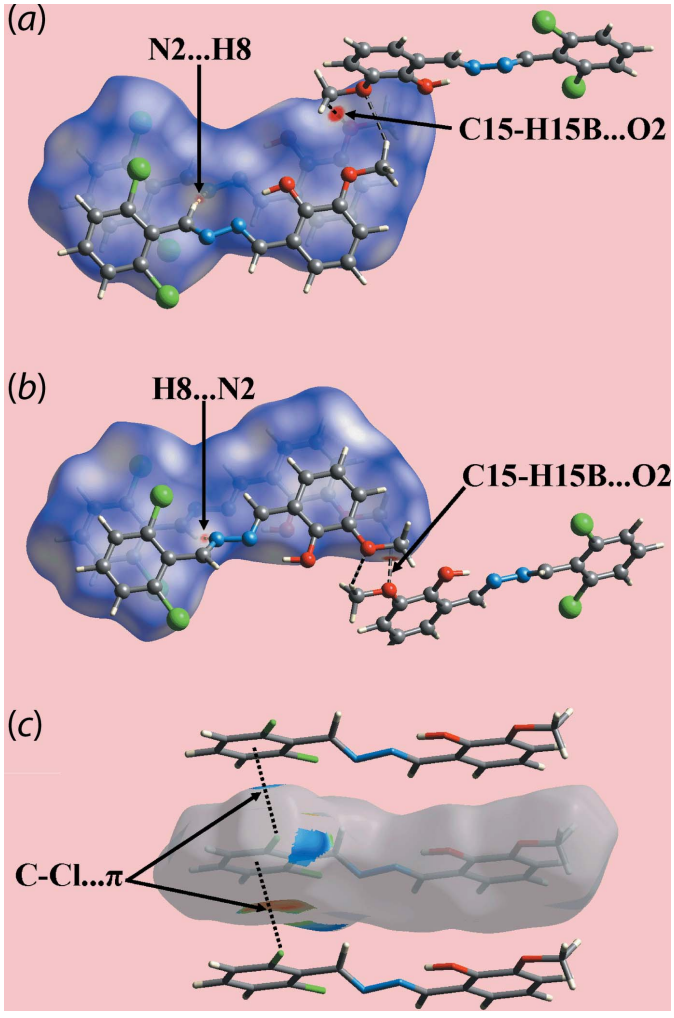

Figure 4
Views of the Hirshfeld surface for (I) mapped: (*a*) and (*b*) over d_{norm} in the range −0.097 to + 1.103 arbitrary units and (*c*) with the shape-index property showing intermolecular C—Cl···π/π···Cl—C contacts.

The overall two-dimensional fingerprint plots for (I), Fig. 7(*a*), and (II), Fig.7(*f*), and those delineated into H···H, O···H/H···O, C···H/H···C and C···C contacts for (I) are illustrated in Fig. 7(*b*)–(*e*), respectively, and the equivalent plots for (II) are found in Fig. 7(*g*)–(*j*). The percentage contributions from the different interatomic contacts to the Hirshfeld surfaces of (I) and (II) are quantitatively summarized in Table 5. For (I), the short interatomic H···H contact between the methoxy-H15*A* and dichlorobenzene-H13 atoms, Table 4, is evident as a pair of almost fused peaks at $d_e + d_i$ ~2.3 Å in Fig.7(*b*). In (II), comparable interactions are at interatomic distances farther than the sum of their van der Waals radii. The decrease in the percentage contribution from H···H contacts to the Hirshfeld surface of (II) compared to (I), Table 5, can be related, in the main, to the presence of the bromine substituent in the hydroxylbenzene ring, in contrast

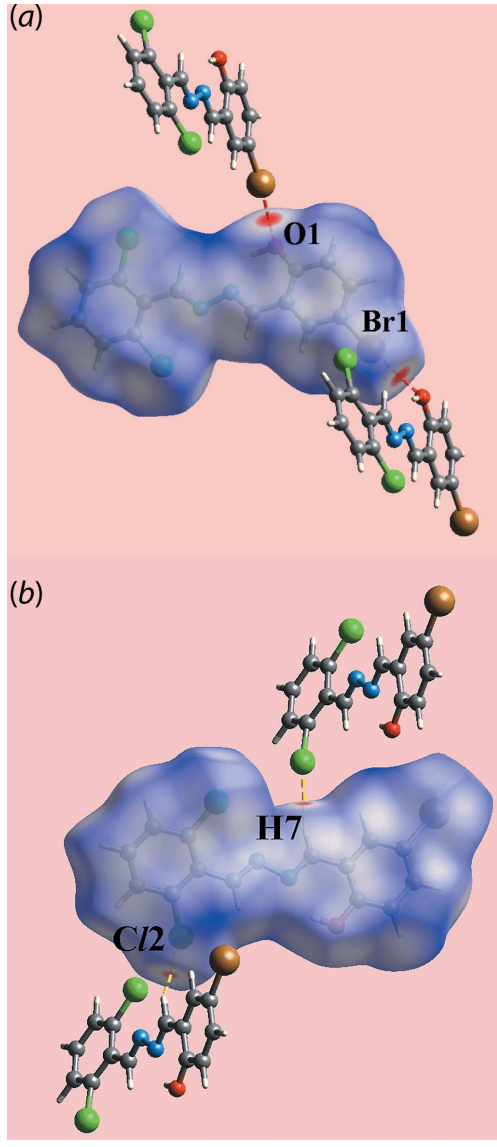

Figure 5
Views of the Hirshfeld surface for (II) mapped over d_{norm} in the range −0.016 to 1.528 arbitrary units.

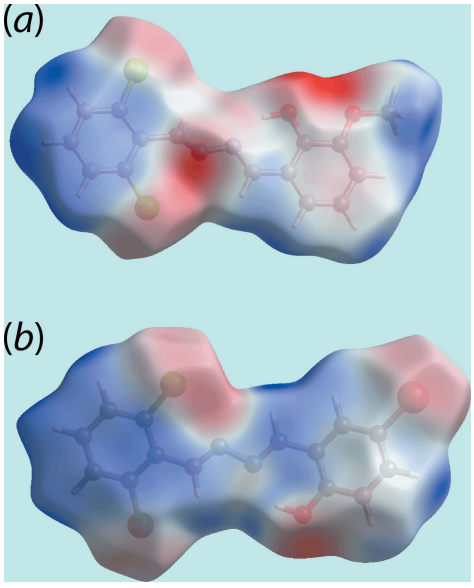

Figure 6
A view of the Hirshfeld surface mapped over the electrostatic potential (the red and blue regions represent negative and positive electrostatic potentials, respectively): (*a*) for (I) in the range −0.071 to +0.038 atomic units and (*b*) for (II) in the range −0.063 to +0.040 atomic units.

Table 5
Percentage contributions of interatomic contacts to the Hirshfeld surface for (I) and (II).

Contact	Percentage contribution	
	(I)	(II)
H···H	31.1	21.1
O···H/H···O	9.1	4.3
C···H/H···C	16.4	13.8
Cl···H/H···Cl	17.3	23.1
N···H/H···N	8.0	0.4
C···Cl/Cl···C	6.2	1.0
C···C	4.6	7.2
C···O/O···C	3.7	0.1
C···N/N···C	0.0	7.1
Cl···Cl	3.5	2.7
Cl···N/N···Cl	0.0	0.6
N···O/O···N	0.0	0.1
Br···H/H···Br	–	13.7
Br···O/O···Br	–	2.6
Br···C/C···Br	–	1.8
Br···Cl/Cl···Br	–	0.2
Br···Br	–	0.2

to the methoxy group in (I), and its participation in a number of surface contacts, most notably Br···H/H···Br contacts (13.7%).

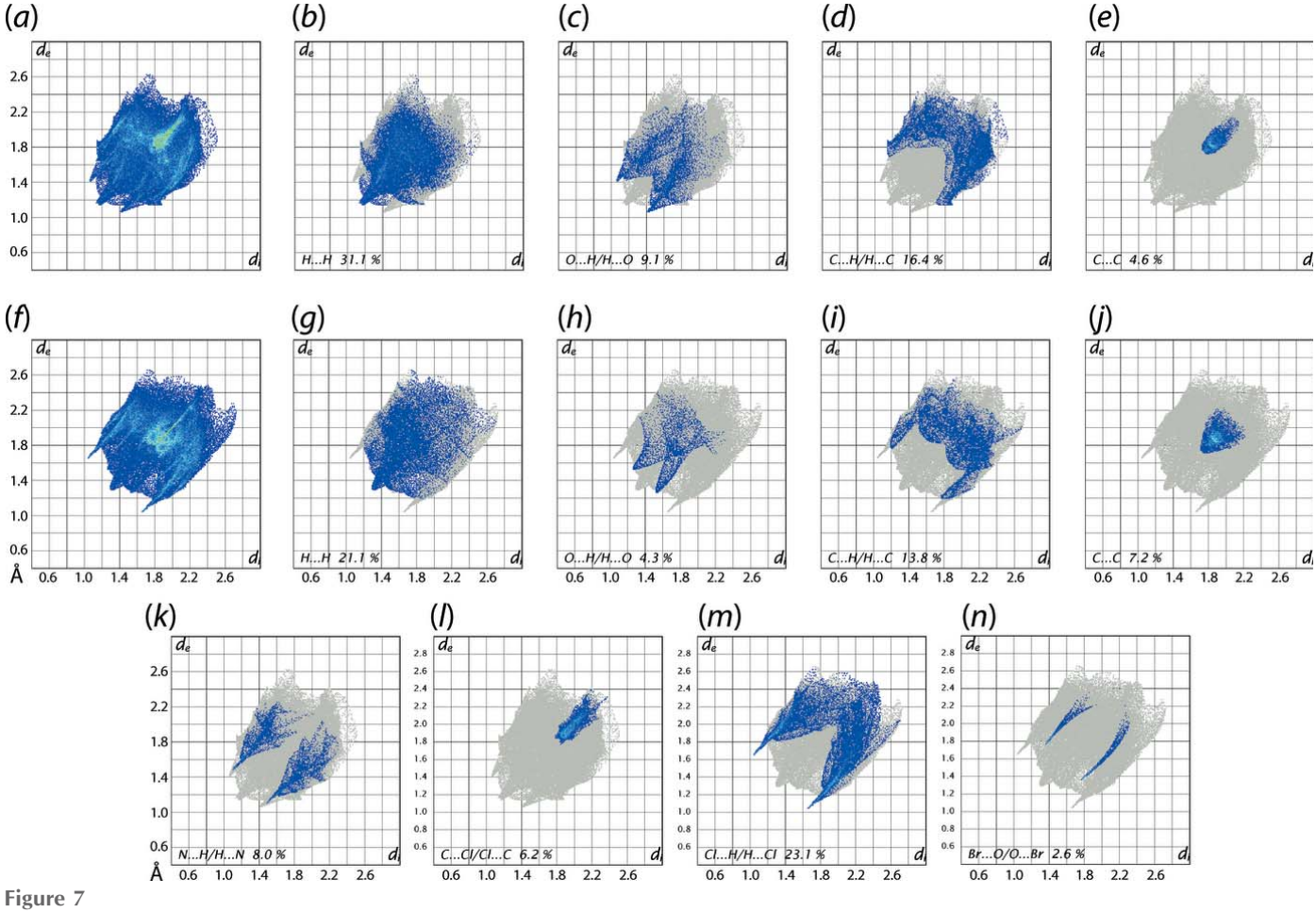

Figure 7
(*a*) A comparison of the full two-dimensional fingerprint plot for (I) and those delineated into (*b*) H···H, (*c*) O···H/H···O, (*d*) C···H/H···C and (*e*) C···C contacts, (*f*)–(*j*) equivalent fingerprint plots for (II), (*g*) N···H/H···N for (I), (*h*) C···Cl/C···Cl for (I), (*i*) Cl···H/H···Cl for (II) and (*j*) Br···O/O···Br for (II).

Table 6
Summary of interaction energies (kJ mol^{-1}) calculated for (I) and (II).

Contact	R (Å)	E_{ele}	E_{pol}	E_{dis}	E_{rep}	E_{tot}
(I)[a]						
C15—H15B···O2^{i}	12.93	−12.5	−2.7	−13.1	9.1	−21.1
C14—Cl2 ···π(C9–C14)^{ii} + N2 ···H8^{iii}	4.36	−4.7	−3.5	−66.8	36.9	−43.0
H13···H15A'^{iv}	13.64	−0.6	−0.6	−9.7	5.5	−6.1
(II)[b]						
Br1···O1^{i}	10.21	−4.6	−0.9	−7.2	5.4	−7.5
Cl2···H7^{ii}	8.69	−3.9	−0.7	−4.2	0.7	−3.1

Notes: (*a*) Symmetry operations for (I): (i) $-1+x, y, z$; (ii) $-\frac{1}{2}+x, \frac{5}{2}-y, -z$; (iii) $1+x, y, z$. (*b*) Symmetry operations for (II): (i) $\frac{1}{2}+x, 3-y, z$; (ii) $-\frac{1}{2}+x, 1-y, z$.

The presence of C—H···O contacts in the crystal of (I) is characterized as the pair of forceps-like tips at $d_e + d_i$ ~2.5 Å in the fingerprint plot delineated into O···H/H···O contacts, Fig. 7(*c*), with the points related to other short interatomic O···H contacts merged within. The comparatively small contribution from these contacts in (II), Table 5, show the points to be at distances greater than sum of their van der Waals radii in Fig. 7(*h*). In the fingerprint plot delineated into C···H/H···C contacts for both (I) and (II), Fig. 7(*d*) and (*i*), the characteristic wings are observed but with different shapes. Their relatively long interatomic distances are consistent with the absence of intermolecular C—H···π or short C···H contacts in the crystals. The absence of aromatic π–π stacking is also evident from the fingerprint plots delineated into C···C contacts, Figs. 7(*e*) and (*j*), although significant percentage contributions from these contacts are noted, Table 5. In addition to the above, some specific contacts occur in the crystals of (I) and (II).

The pair of forceps-like tips at $d_e + d_i$ ~2.5 Å in the fingerprint plot delineated into N···H/H···N contacts for (I) in Fig. 7(*k*) indicate the short interatomic N···H contact involving the imine-N2 and H12 atoms, Table 4, formed within the supramolecular chain along *a* axis Fig. 2(*a*). Also, in the fingerprint plot delineated into C···Cl/Cl···C contacts for (I), Fig. 7(*l*), the C—Cl···π contacts are highlighted as the pattern of blue points at separations as close as $d_e = d_i = 1.85$ Å. In the case of (II), in the fingerprint plot delineated into Cl···H/H···Cl contacts, Fig. 7(*m*), the short interatomic contact involving the Cl2 and imine-H7 atoms is apparent as the pair of spikes with their tips at $d_e + d_i$ ~2.7 Å. Finally, the presence of interatomic Br···O interactions along the *a* axis in the crystal is reflected in the pair of thin spikes at $d_e + d_i$ ~3.2 Å in Fig. 7(*n*). The comparatively greater percentage contribution from interatomic contacts such as C···O/O···C and Cl···Cl to the surface of (I) and Br···H/H···Br and C···N/N···C to that of (II) as well as smaller contributions from other contacts as summarized in Table 5, show negligible effect on the respective molecular packing due to the interatomic separations being equal to or exceeding the respective sums of the van der Waals radii.

5. Energy frameworks

The pairwise interaction energies between the molecules in the crystals of (I) and (II) were calculated by summing up four energy components, these being the electrostatic (E_{ele}), polarization (E_{pol}), dispersion (E_{dis}) and exchange-repulsion (E_{rep}) terms (Turner *et al.*, 2017). The energies were obtained using the wavefunctions calculated at the B3LYP/6–31 G(*d*,*p*) and HF/STO-3 G levels theory for (I) and (II), respectively. The individual energy components as well as the total interaction energy were calculated relative to a reference molecule. The nature and strength of the energies for the key identified intermolecular interactions are summarized in Table 6.

It is apparent from the interaction energies calculated for (I) that the dispersion component, E_{dis}, makes the major contribution to the C—Cl···π and N···H contacts and these are dominant in the molecular packing. By contrast, the C—H···O interaction has nearly equal contributions from the electrostatic component, E_{ele}, and E_{dis}. The small value of the interaction energy corresponding to the short H···H contact arises primarily from E_{dis}. The intermolecular Br···O and Cl···H contacts instrumental in the crystal of (II) have small interaction energy values dominated by E_{dis}.

Fig. 8 represents graphically the magnitudes of intermolecular energies in the form of energy frameworks, which provide a view of the supramolecular architecture of crystals

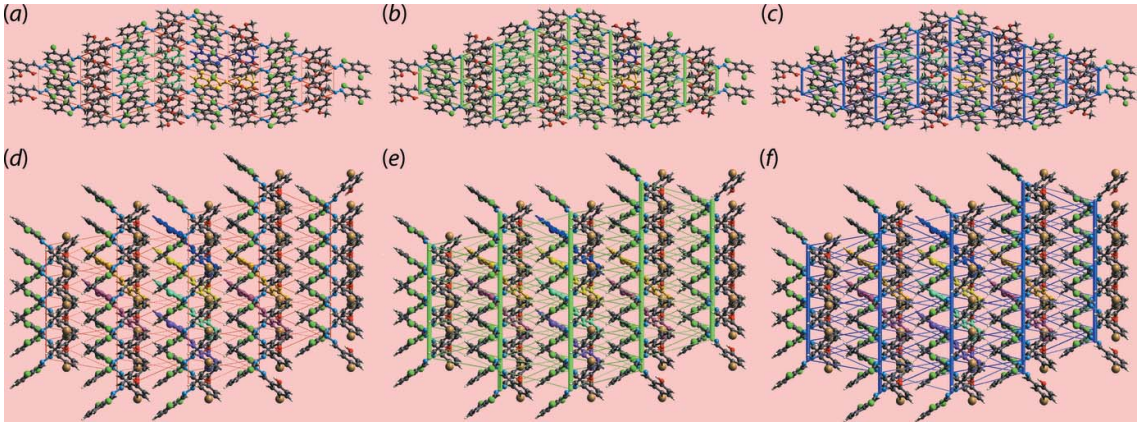

Figure 8
The energy frameworks calculated for (I) showing the (*a*) electrostatic potential force, (*b*) dispersion force and (*c*) total energy. The energy frameworks were adjusted to the same scale factor of 50 with a cut-off value of 3 kJ mol^{-1} within 4 × 4 × 4 unit cells. (*d*)–(*f*) Equivalent frameworks for (II).

Table 7
Experimental details.

	(I)	(II)
Crystal data		
Chemical formula	$C_{15}H_{12}Cl_2N_2O_2$	$C_{14}H_9BrCl_2N_2O$
M_r	323.17	372.04
Crystal system, space group	Orthorhombic, $P2_12_12_1$	Orthorhombic, $Pca2_1$
Temperature (K)	296	296
a, b, c (Å)	4.3556 (2), 12.8548 (4), 25.9904 (9)	16.4510 (12), 4.4314 (3), 20.0523 (15)
V (Å^3)	1455.21 (10)	1461.83 (18)
Z	4	4
Radiation type	Mo $K\alpha$	Mo $K\alpha$
μ (mm^{-1})	0.45	3.17
Crystal size (mm)	0.30 × 0.25 × 0.25	0.30 × 0.20 × 0.20
Data collection		
Diffractometer	Bruker Kappa APEXII CCD	Bruker Kappa APEXII CCD
Absorption correction	Multi-scan (*SADABS*; Bruker, 2004)	Multi-scan (*SADABS*; Bruker, 2004)
T_{min}, T_{max}	0.557, 0.746	0.398, 0.746
No. of measured, independent and observed [$I > 2\sigma(I)$] reflections	48935, 3751, 2909	39831, 3569, 2150
R_{int}	0.070	0.108
(sin $\theta/\lambda)_{max}$ (Å^{-1})	0.678	0.666
Refinement		
$R[F^2 > 2\sigma(F^2)]$, $wR(F^2)$, S	0.039, 0.099, 1.02	0.038, 0.082, 1.00
No. of reflections	3751	3569
No. of parameters	194	184
No. of restraints	1	2
H-atom treatment	H atoms treated by a mixture of independent and constrained refinement	H atoms treated by a mixture of independent and constrained refinement
$\Delta\rho_{max}$, $\Delta\rho_{min}$ (e Å^{-3})	0.16, −0.25	0.30, −0.59
Absolute structure	Flack x determined using 1004 quotients $[(I^+)-(I^-)]/[(I^+)+(I^-)]$ (Parsons *et al.*, 2013).	Flack x determined using 829 quotients $[(I^+)-(I^-)]/[(I^+)+(I^-)]$ (Parsons *et al.*, 2013).
Absolute structure parameter	0.12 (3)	0.003 (7)

Computer programs: *APEX2* and *SAINT* (Bruker, 2004), *SIR92* (Altomare *et al.*, 1994), *SHELXL2014/7* (Sheldrick, 2015), *ORTEP-3 for Windows* (Farrugia, 2012), *DIAMOND* (Brandenburg, 2006) and *publCIF* (Westrip, 2010).

through cylinders joining centroids of molecular pairs by using red, green and blue colour codes for the components E_{ele}, E_{disp} and E_{tot}, respectively. The radius of the cylinder is proportional to the magnitude of the interaction energies which are adjusted to same scale factor of 50 with a cut-off value of 3 kJ mol^{-1} within 4 × 4 × 4 unit cells. The appearance of the energy frameworks clearly reflect the foregoing discussion, namely the clear dominance of the E_{dis} terms, especially for (II).

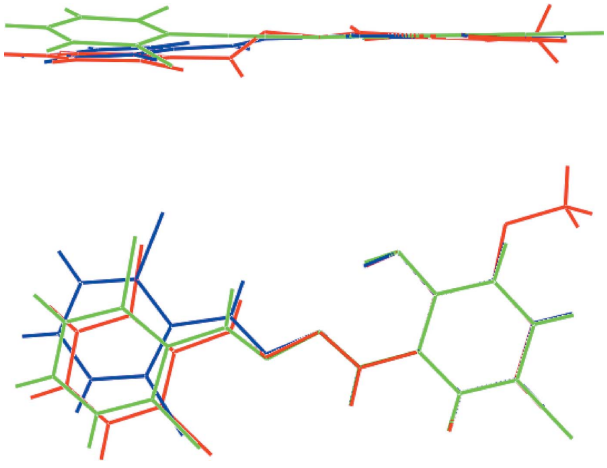

Figure 9
Two overlay diagrams of (I)–(III), represented by red, green and blue images, respectively. The molecules have been overlapped so the O1, N1 and C1 atoms are coincident.

6. Database survey

In a recent contribution describing the structure of the analogue of (I) where the methoxy substituent is absent (Manawar *et al.*, 2019*b*), *i.e.* (III), it was noted that crystal structure determinations of molecules with the 2-OH-C_6-C(H)N—NC(H)-C_6 fragment number fewer than ten, and that there is some conformational flexibility in these molecules. This observation is borne out in the present study where there is a disparity of over 25° in the central C7—N1—N2—C8 torsion angle, *i.e.* −151.0 (3) and 177.8 (6)° for (I) and (II), respectively. These values compare with the equivalent angle of −172.7 (2)° in (III). An overlay diagram for (I)–(III) is shown in Fig. 9: here, the different conformations for (I), *cf.* (II) and (III), are clearly evident.

7. Synthesis and crystallization

The title compounds were synthesized and characterized as per the procedures reported in the literature (Manawar *et al.*, 2019*a*). The crystals of (I) and (II) in the form of yellow blocks suitable for the structural study reported here were grown by slow evaporation of their chloroform solutions.

8. Refinement

Crystal data, data collection and structure refinement details are summarized in Table 7. Carbon-bound H atoms were placed in calculated positions (C—H = 0.93–0.96 Å) and were included in the refinement in the riding-model approximation, with U_{iso}(H) set to 1.2–1.5U_{eq}(C). The positions of the O-bound H atoms were refined with O—H = 0.82±0.01 Å, and with U_{iso}(H) set to 1.5U_{eq}(O).

Acknowledgements

The authors thank the Department of Chemistry, Saurashtra University, Rajkot, Gujarat, India, for access to the chemical synthesis laboratory and to the Sophisticated Analytical Instrumentation Centre (SAIC), Tezpur, Assam, India for providing the X-ray intensity data for (I) and (II).

Funding information

Crystallographic research at Sunway University is supported by Sunway University Sdn Bhd (grant No. STR-RCTR-RCCM-001-2019).

References

Alcock, N. W. (1972). *Adv. Inorg. Chem. Radiochem.* **15**, 1–58.

Altomare, A., Cascarano, G., Giacovazzo, C., Guagliardi, A., Burla, M. C., Polidori, G. & Camalli, M. (1994). *J. Appl. Cryst.* **27**, 435.

Brandenburg, K. (2006). *DIAMOND*. Crystal Impact GbR, Bonn, Germany.

Bruker (2004). *APEX2*, *SAINT* and *SADABS*. Bruker AXS Inc., Madison, Wisconsin, USA.

Clarke, R. M. & Storr, T. (2014). *Dalton Trans.* **43**, 9380–9391.

Farrugia, L. J. (2012). *J. Appl. Cryst.* **45**, 849–854.

Hassel, O. & Hvoslef, J. (1954). *Acta Chem. Scand.* **8**, 873.

Liu, X., Manzur, C., Novoa, N., Celedón, S., Carrillo, D. & Hamon, J.-R. (2018). *Coord. Chem. Rev.* **357**, 144–172.

Manawar, R. B., Gondaliya, M. B., Mamtora, M. J. & Shah, M. K. (2019*a*). *Sci. News* 126, 222–247.

Manawar, R. B., Gondaliya, M. B., Shah, M. K., Jotani, M. M. & Tiekink, E. R. T. (2019*b*). *Acta Cryst.* E**75**, 1423–1428.

Manawar, R. B., Mamtora, M. J., Shah, M. K., Jotani, M. M. & Tiekink, E. R. T. (2020). *Acta Cryst.* E**76**, 53–61.

Mukherjee, T., Pessoa, J. C., Kumar, A. & Sarkar, A. R. (2013). *Dalton Trans.* **42**, 2594–2607.

Naeimi, H., Nazifi, Z. S., Matin Amininezhad, S. & Amouheidari, M. (2013). *J. Antibiot.* **66**, 687–689.

Parsons, S., Flack, H. D. & Wagner, T. (2013). *Acta Cryst.* B**69**, 249–259.

Sheldrick, G. M. (2015). *Acta Cryst.* C**71**, 3–8.

Tan, S. L., Jotani, M. M. & Tiekink, E. R. T. (2019). *Acta Cryst.* E**75**, 308–318.

Tiekink, E. R. T. (2017). *Coord. Chem. Rev*. **345**, 219–228.

Turner, M. J., Mckinnon, J. J., Wolff, S. K., Grimwood, D. J., Spackman, P. R., Jayatilaka, D. & Spackman, M. A. (2017). Crystal Explorer v17. The University of Western Australia.

Vigato, P. A. & Tamburini, S. (2004). *Coord. Chem. Rev.* **248**, 1717–2128.

Westrip, S. P. (2010). *J. Appl. Cryst.* **43**, 920–925.

supporting information

Acta Cryst. (2020). E**76**, 862-869 [https://doi.org/10.1107/S2056989020006416]

Crystal structures of two dis-symmetric di-Schiff base compounds: 2-({(*E*)-2-[(*E*)-2,6-dichlorobenzylidene]hydrazin-1-ylidene}methyl)-6-methoxyphenol and 4-bromo-2-({(*E*)-2-[(*E*)-2,6-dichlorobenzylidene]hydrazin-1-ylidene}methyl)phenol

Rohit B. Manawar, Chandankumar T. Pashavan, Manish K. Shah, Mukesh M. Jotani and Edward R. T. Tiekink

Computing details

For both structures, data collection: *APEX2* (Bruker, 2004); cell refinement: *APEX2*/*SAINT* (Bruker, 2004); data reduction: *SAINT* (Bruker, 2004); program(s) used to solve structure: *SIR92* (Altomare *et al.*, 1994); program(s) used to refine structure: *SHELXL2014/7* (Sheldrick, 2015); molecular graphics: *ORTEP-3 for Windows* (Farrugia, 2012), *DIAMOND* (Brandenburg, 2006); software used to prepare material for publication: *publCIF* (Westrip, 2010).

2-({(*E*)-2-[(*E*)-2,6-Dichlorobenzylidene]hydrazin-1-ylidene}methyl)-6-methoxyphenol (I)

Crystal data

$C_{15}H_{12}Cl_2N_2O_2$
M_r = 323.17
Orthorhombic, $P2_12_12_1$
a = 4.3556 (2) Å
b = 12.8548 (4) Å
c = 25.9904 (9) Å
V = 1455.21 (10) Å^3
Z = 4
$F(000)$ = 664
D_x = 1.475 Mg m^{-3}
Mo $K\alpha$ radiation, λ = 0.71073 Å
Cell parameters from 7669 reflections
θ = 2.8–20.9°
μ = 0.45 mm^{-1}
T = 296 K
Block, yellow
0.30 × 0.25 × 0.25 mm

Data collection

Bruker Kappa APEXII CCD diffractometer
Radiation source: X-ray tube
ω and φ scan
Absorption correction: multi-scan (SADABS; Bruker, 2004)
T_{min} = 0.557, T_{max} = 0.746
48935 measured reflections
3751 independent reflections
2909 reflections with $I > 2\sigma(I)$
R_{int} = 0.070
θ_{max} = 28.8°, θ_{min} = 1.6°
h = −5→5
k = −17→17
l = −34→35

Refinement

Refinement on F^2
Least-squares matrix: full
$R[F^2 > 2\sigma(F^2)]$ = 0.039
$wR(F^2)$ = 0.099
S = 1.02
3751 reflections
194 parameters
1 restraint
Primary atom site location: structure-invariant direct methods

Secondary atom site location: difference Fourier map
Hydrogen site location: mixed
H atoms treated by a mixture of independent and constrained refinement
$w = 1/[\sigma^2(F_o^2) + (0.0465P)^2 + 0.2295P]$ where $P = (F_o^2 + 2F_c^2)/3$
$(\Delta/\sigma)_{max} < 0.001$
$\Delta\rho_{max} = 0.16$ e Å^{-3}
$\Delta\rho_{min} = -0.25$ e Å^{-3}
Absolute structure: Flack *x* determined using 1004 quotients $[(I^+)-(I^-)]/[(I^+)+(I^-)]$ (Parsons *et al.*, 2013).
Absolute structure parameter: 0.12 (3)

Special details

Geometry. All esds (except the esd in the dihedral angle between two l.s. planes) are estimated using the full covariance matrix. The cell esds are taken into account individually in the estimation of esds in distances, angles and torsion angles; correlations between esds in cell parameters are only used when they are defined by crystal symmetry. An approximate (isotropic) treatment of cell esds is used for estimating esds involving l.s. planes.

Fractional atomic coordinates and isotropic or equivalent isotropic displacement parameters (Å²)

	x	*y*	*z*	U_{iso}*/U_{eq}
Cl1	0.5635 (2)	0.58257 (6)	0.17813 (3)	0.0639 (2)
Cl2	−0.1091 (2)	0.85695 (7)	0.29187 (3)	0.0635 (2)
O1	0.0486 (6)	1.03357 (16)	0.07165 (7)	0.0526 (5)
H1O	0.076 (10)	0.990 (2)	0.0947 (10)	0.079*
O2	−0.0282 (6)	1.13830 (16)	−0.01337 (7)	0.0580 (6)
N1	0.2888 (6)	0.86954 (18)	0.11908 (9)	0.0462 (6)
N2	0.3817 (6)	0.80405 (19)	0.15969 (9)	0.0511 (6)
C1	0.3847 (6)	0.9094 (2)	0.03056 (9)	0.0407 (6)
C2	0.1975 (6)	0.9977 (2)	0.02967 (9)	0.0406 (6)
C3	0.1588 (7)	1.0536 (2)	−0.01676 (10)	0.0436 (6)
C4	0.3053 (7)	1.0193 (2)	−0.06085 (10)	0.0529 (8)
H4	0.280990	1.055923	−0.091441	0.063*
C5	0.4876 (8)	0.9312 (3)	−0.05996 (11)	0.0577 (8)
H5	0.581625	0.908278	−0.090022	0.069*
C6	0.5300 (8)	0.8777 (2)	−0.01501 (11)	0.0531 (7)
H6	0.656910	0.819478	−0.014652	0.064*
C7	0.4354 (7)	0.8510 (2)	0.07726 (10)	0.0454 (6)
H7	0.580111	0.797798	0.077020	0.054*
C8	0.1755 (7)	0.7862 (2)	0.19229 (10)	0.0433 (6)
H8	−0.017552	0.815862	0.188063	0.052*
C9	0.2348 (6)	0.7189 (2)	0.23722 (10)	0.0384 (6)
C10	0.4098 (7)	0.6277 (2)	0.23543 (10)	0.0442 (6)
C11	0.4597 (8)	0.5674 (2)	0.27870 (12)	0.0559 (8)
H11	0.578168	0.507359	0.276454	0.067*
C12	0.3337 (8)	0.5965 (3)	0.32511 (12)	0.0597 (8)
H12	0.370349	0.556547	0.354312	0.072*
C13	0.1540 (8)	0.6841 (3)	0.32858 (11)	0.0543 (8)
H13	0.064794	0.702856	0.359734	0.065*
C14	0.1081 (7)	0.7439 (2)	0.28499 (10)	0.0439 (6)
C15	−0.0503 (10)	1.2040 (3)	−0.05738 (12)	0.0743 (11)
H15A	0.146096	1.235029	−0.064168	0.111*
H15B	−0.198696	1.257741	−0.051006	0.111*

H15C	−0.113212	1.163644	−0.086601	0.111*

Atomic displacement parameters (Å²)

	U^{11}	U^{22}	U^{33}	U^{12}	U^{13}	U^{23}
Cl1	0.0822 (6)	0.0538 (4)	0.0555 (4)	0.0136 (4)	0.0063 (4)	−0.0055 (4)
Cl2	0.0727 (5)	0.0550 (4)	0.0628 (5)	0.0050 (4)	0.0086 (4)	−0.0072 (4)
O1	0.0699 (14)	0.0525 (12)	0.0353 (10)	0.0110 (11)	0.0077 (10)	0.0009 (8)
O2	0.0781 (15)	0.0535 (12)	0.0425 (11)	0.0107 (12)	0.0016 (10)	0.0082 (9)
N1	0.0520 (14)	0.0456 (13)	0.0412 (13)	−0.0021 (11)	−0.0001 (11)	0.0106 (10)
N2	0.0489 (13)	0.0557 (14)	0.0486 (13)	0.0001 (12)	−0.0027 (12)	0.0156 (11)
C1	0.0438 (14)	0.0426 (14)	0.0356 (13)	−0.0066 (12)	0.0008 (11)	−0.0029 (11)
C2	0.0476 (15)	0.0438 (14)	0.0303 (12)	−0.0066 (12)	0.0019 (11)	−0.0054 (11)
C3	0.0493 (15)	0.0448 (15)	0.0366 (13)	−0.0063 (13)	−0.0020 (12)	−0.0002 (11)
C4	0.0604 (19)	0.066 (2)	0.0325 (14)	−0.0094 (16)	0.0021 (13)	0.0015 (14)
C5	0.064 (2)	0.0714 (19)	0.0377 (15)	−0.0019 (18)	0.0109 (14)	−0.0091 (14)
C6	0.0553 (17)	0.0555 (17)	0.0484 (16)	−0.0004 (15)	0.0075 (14)	−0.0117 (13)
C7	0.0469 (16)	0.0408 (14)	0.0485 (15)	−0.0024 (13)	−0.0020 (13)	0.0001 (12)
C8	0.0494 (16)	0.0414 (14)	0.0390 (14)	−0.0027 (13)	−0.0062 (12)	0.0021 (11)
C9	0.0406 (13)	0.0377 (13)	0.0370 (13)	−0.0076 (11)	−0.0051 (11)	0.0022 (10)
C10	0.0472 (15)	0.0433 (14)	0.0420 (14)	−0.0030 (13)	−0.0037 (13)	0.0007 (12)
C11	0.0602 (18)	0.0476 (16)	0.0600 (18)	0.0029 (15)	−0.0070 (15)	0.0143 (14)
C12	0.066 (2)	0.065 (2)	0.0481 (17)	−0.0039 (17)	−0.0051 (16)	0.0233 (15)
C13	0.0587 (18)	0.069 (2)	0.0355 (14)	−0.0093 (16)	−0.0006 (13)	0.0059 (14)
C14	0.0456 (15)	0.0442 (14)	0.0419 (14)	−0.0082 (12)	−0.0026 (13)	−0.0016 (12)
C15	0.098 (3)	0.072 (2)	0.0529 (19)	0.014 (2)	−0.001 (2)	0.0195 (17)

Geometric parameters (Å, º)

Cl1—C10	1.733 (3)	C5—H5	0.9300
Cl2—C14	1.743 (3)	C6—H6	0.9300
O1—C2	1.350 (3)	C7—H7	0.9300
O1—H1O	0.828 (13)	C8—C9	1.476 (4)
O2—C3	1.362 (4)	C8—H8	0.9300
O2—C15	1.425 (3)	C9—C10	1.399 (4)
N1—C7	1.283 (3)	C9—C14	1.396 (4)
N1—N2	1.409 (3)	C10—C11	1.383 (4)
N2—C8	1.256 (4)	C11—C12	1.377 (4)
C1—C2	1.398 (4)	C11—H11	0.9300
C1—C6	1.403 (4)	C12—C13	1.374 (5)
C1—C7	1.444 (4)	C12—H12	0.9300
C2—C3	1.415 (4)	C13—C14	1.384 (4)
C3—C4	1.384 (4)	C13—H13	0.9300
C4—C5	1.383 (4)	C15—H15A	0.9600
C4—H4	0.9300	C15—H15B	0.9600
C5—C6	1.369 (4)	C15—H15C	0.9600
C2—O1—H1O	107 (3)	N2—C8—H8	119.5

C3—O2—C15	117.5 (3)	C9—C8—H8	119.5
C7—N1—N2	112.4 (2)	C10—C9—C14	116.0 (2)
C8—N2—N1	114.2 (2)	C10—C9—C8	124.1 (2)
C2—C1—C6	119.0 (3)	C14—C9—C8	120.0 (3)
C2—C1—C7	121.7 (2)	C11—C10—C9	121.9 (3)
C6—C1—C7	119.3 (3)	C11—C10—Cl1	116.8 (2)
O1—C2—C1	123.0 (2)	C9—C10—Cl1	121.3 (2)
O1—C2—C3	117.3 (3)	C10—C11—C12	119.8 (3)
C1—C2—C3	119.8 (2)	C10—C11—H11	120.1
O2—C3—C4	125.7 (3)	C12—C11—H11	120.1
O2—C3—C2	115.0 (2)	C13—C12—C11	120.5 (3)
C4—C3—C2	119.3 (3)	C13—C12—H12	119.8
C3—C4—C5	120.8 (3)	C11—C12—H12	119.8
C3—C4—H4	119.6	C12—C13—C14	118.9 (3)
C5—C4—H4	119.6	C12—C13—H13	120.5
C6—C5—C4	120.2 (3)	C14—C13—H13	120.5
C6—C5—H5	119.9	C13—C14—C9	122.9 (3)
C4—C5—H5	119.9	C13—C14—Cl2	117.3 (2)
C5—C6—C1	120.9 (3)	C9—C14—Cl2	119.8 (2)
C5—C6—H6	119.5	O2—C15—H15A	109.5
C1—C6—H6	119.5	O2—C15—H15B	109.5
N1—C7—C1	122.6 (3)	H15A—C15—H15B	109.5
N1—C7—H7	118.7	O2—C15—H15C	109.5
C1—C7—H7	118.7	H15A—C15—H15C	109.5
N2—C8—C9	121.1 (3)	H15B—C15—H15C	109.5

C7—N1—N2—C8	−151.0 (3)	C6—C1—C7—N1	−173.4 (3)
C6—C1—C2—O1	179.9 (3)	N1—N2—C8—C9	179.9 (2)
C7—C1—C2—O1	−1.0 (4)	N2—C8—C9—C10	−39.5 (4)
C6—C1—C2—C3	−0.3 (4)	N2—C8—C9—C14	141.8 (3)
C7—C1—C2—C3	178.8 (3)	C14—C9—C10—C11	−1.4 (4)
C15—O2—C3—C4	−7.2 (5)	C8—C9—C10—C11	179.7 (3)
C15—O2—C3—C2	173.5 (3)	C14—C9—C10—Cl1	176.3 (2)
O1—C2—C3—O2	−0.2 (4)	C8—C9—C10—Cl1	−2.5 (4)
C1—C2—C3—O2	180.0 (2)	C9—C10—C11—C12	0.4 (5)
O1—C2—C3—C4	−179.6 (3)	Cl1—C10—C11—C12	−177.4 (2)
C1—C2—C3—C4	0.6 (4)	C10—C11—C12—C13	1.1 (5)
O2—C3—C4—C5	−179.2 (3)	C11—C12—C13—C14	−1.5 (5)
C2—C3—C4—C5	0.1 (4)	C12—C13—C14—C9	0.5 (4)
C3—C4—C5—C6	−1.2 (5)	C12—C13—C14—Cl2	−177.6 (3)
C4—C5—C6—C1	1.5 (5)	C10—C9—C14—C13	1.0 (4)
C2—C1—C6—C5	−0.8 (4)	C8—C9—C14—C13	179.9 (3)
C7—C1—C6—C5	−179.9 (3)	C10—C9—C14—Cl2	179.0 (2)
N2—N1—C7—C1	−178.8 (2)	C8—C9—C14—Cl2	−2.1 (4)
C2—C1—C7—N1	7.5 (4)		

Hydrogen-bond geometry (Å, º)

*Cg*1 is the centroid of the (C9–14) ring.

D—H···*A*	*D*—H	H···*A*	*D*···*A*	*D*—H···*A*
O1—H1*O*···N1	0.83 (3)	1.91 (3)	2.657 (3)	149 (3)
C15—H15*B*···O2^{i}	0.96	2.58	3.439 (4)	149
C14—Cl2···*Cg*1^{ii}	1.74 (1)	3.70 (1)	3.765 (3)	79 (1)

Symmetry codes: (i) *x*−1/2, −*y*+5/2, −*z*; (ii) *x*−1, *y*, *z*.

4-Bromo-2-({(*E*)-2-[(*E*)-2,6-dichlorobenzylidene]hydrazin-1-ylidene}methyl)phenol (II)

Crystal data

$C_{14}H_9BrCl_2N_2O$
M_r = 372.04
Orthorhombic, $Pca2_1$
a = 16.4510 (12) Å
b = 4.4314 (3) Å
c = 20.0523 (15) Å
V = 1461.83 (18) Å^3
Z = 4
F(000) = 736
D_x = 1.690 Mg m^{-3}
Mo $K\alpha$ radiation, λ = 0.71073 Å
Cell parameters from 4698 reflections
θ = 2.5–18.6°
μ = 3.17 mm^{-1}
T = 296 K
Block, yellow
0.30 × 0.20 × 0.20 mm

Data collection

Bruker Kappa APEXII CCD diffractometer
Radiation source: X-ray tube
ω and φ scan
Absorption correction: multi-scan (SADABS; Bruker, 2004)
T_{min} = 0.398, T_{max} = 0.746
39831 measured reflections
3569 independent reflections
2150 reflections with $I > 2\sigma(I)$
R_{int} = 0.108
θ_{max} = 28.3°, θ_{min} = 2.5°
h = −21→21
k = −5→5
l = −26→26

Refinement

Refinement on F^2
Least-squares matrix: full
$R[F^2 > 2\sigma(F^2)]$ = 0.038
$wR(F^2)$ = 0.082
S = 1.00
3569 reflections
184 parameters
2 restraints
Primary atom site location: structure-invariant direct methods
Secondary atom site location: difference Fourier map
Hydrogen site location: mixed
H atoms treated by a mixture of independent and constrained refinement
$w = 1/[\sigma^2(F_o^2) + (0.024P)^2 + 0.3263P]$ where $P = (F_o^2 + 2F_c^2)/3$
$(\Delta/\sigma)_{max} < 0.001$
$\Delta\rho_{max}$ = 0.30 e Å^{-3}
$\Delta\rho_{min}$ = −0.59 e Å^{-3}
Absolute structure: Flack x determined using 829 quotients $[(I^+)-(I^-)]/[(I^+)+(I^-)]$ (Parsons *et al.*, 2013).
Absolute structure parameter: 0.003 (7)

Special details

Geometry. All esds (except the esd in the dihedral angle between two l.s. planes) are estimated using the full covariance matrix. The cell esds are taken into account individually in the estimation of esds in distances, angles and torsion angles; correlations between esds in cell parameters are only used when they are defined by crystal symmetry. An approximate (isotropic) treatment of cell esds is used for estimating esds involving l.s. planes.

Fractional atomic coordinates and isotropic or equivalent isotropic displacement parameters (Å²)

	x	*y*	*z*	U_{iso}*/U_{eq}
Br1	1.17606 (4)	1.58575 (14)	0.09985 (4)	0.0617 (2)
Cl1	0.95249 (10)	0.2117 (4)	0.37299 (9)	0.0682 (5)
Cl2	0.63270 (11)	0.3504 (5)	0.30362 (11)	0.0830 (6)
O1	0.8392 (2)	1.0502 (9)	0.1011 (4)	0.0618 (10)
H1O	0.830 (5)	0.931 (14)	0.132 (3)	0.093*
N1	0.8804 (3)	0.7671 (11)	0.2128 (2)	0.0459 (12)
N2	0.8764 (3)	0.5871 (12)	0.2711 (3)	0.0583 (14)
C1	0.9706 (3)	1.0963 (12)	0.1535 (3)	0.0395 (13)
C2	0.9148 (3)	1.1674 (11)	0.1024 (4)	0.0461 (13)
C3	0.9379 (4)	1.3636 (14)	0.0523 (3)	0.0568 (18)
H3	0.901334	1.412779	0.018641	0.068*
C4	1.0152 (4)	1.4872 (14)	0.0519 (3)	0.0557 (17)
H4	1.029972	1.620146	0.018149	0.067*
C5	1.0700 (3)	1.4155 (11)	0.1008 (5)	0.0454 (12)
C6	1.0480 (4)	1.2229 (13)	0.1514 (3)	0.0450 (15)
H6	1.085312	1.176591	0.184695	0.054*
C7	0.9496 (4)	0.8944 (13)	0.2077 (3)	0.0458 (14)
H7	0.988542	0.855756	0.240209	0.055*
C8	0.8102 (4)	0.4636 (14)	0.2809 (3)	0.0490 (15)
H8	0.769260	0.494996	0.249745	0.059*
C9	0.7918 (4)	0.2707 (15)	0.3384 (3)	0.0441 (15)
C10	0.8495 (4)	0.1490 (13)	0.3823 (3)	0.0471 (15)
C11	0.8267 (4)	−0.0303 (14)	0.4358 (3)	0.0602 (17)
H11	0.866252	−0.109704	0.463911	0.072*
C12	0.7460 (5)	−0.0916 (16)	0.4478 (4)	0.073 (2)
H12	0.731322	−0.211614	0.483867	0.087*
C13	0.6868 (4)	0.0252 (16)	0.4062 (4)	0.066 (2)
H13	0.632125	−0.015359	0.413876	0.079*
C14	0.7104 (4)	0.2044 (17)	0.3525 (3)	0.0525 (18)

Atomic displacement parameters (Å²)

	U^{11}	U^{22}	U^{33}	U^{12}	U^{13}	U^{23}
Br1	0.0534 (4)	0.0635 (3)	0.0682 (4)	−0.0060 (3)	0.0127 (4)	−0.0003 (5)
Cl1	0.0462 (9)	0.0986 (13)	0.0599 (10)	0.0036 (9)	−0.0082 (8)	0.0084 (10)
Cl2	0.0440 (10)	0.1108 (15)	0.0943 (14)	−0.0090 (11)	−0.0136 (10)	0.0087 (13)
O1	0.048 (2)	0.068 (3)	0.069 (3)	−0.003 (2)	−0.015 (3)	0.010 (3)
N1	0.047 (3)	0.044 (3)	0.047 (3)	0.000 (3)	−0.004 (2)	−0.001 (2)
N2	0.048 (4)	0.067 (4)	0.060 (4)	−0.011 (3)	−0.011 (3)	0.019 (3)
C1	0.043 (3)	0.036 (3)	0.039 (3)	0.003 (3)	0.001 (3)	−0.004 (3)
C2	0.046 (3)	0.044 (3)	0.048 (3)	0.005 (2)	−0.005 (4)	−0.001 (4)
C3	0.063 (5)	0.054 (4)	0.053 (4)	0.009 (3)	−0.013 (3)	0.005 (3)
C4	0.068 (5)	0.049 (4)	0.050 (4)	0.001 (3)	0.004 (4)	0.009 (3)
C5	0.053 (3)	0.038 (3)	0.045 (3)	0.003 (3)	0.006 (4)	−0.003 (4)
C6	0.043 (4)	0.046 (3)	0.046 (4)	0.004 (3)	−0.001 (3)	−0.002 (3)

C7	0.042 (4)	0.049 (3)	0.047 (3)	0.004 (3)	−0.005 (3)	0.002 (3)
C8	0.041 (4)	0.059 (4)	0.047 (4)	0.002 (3)	−0.007 (3)	0.000 (3)
C9	0.044 (4)	0.046 (4)	0.042 (4)	−0.008 (3)	−0.001 (3)	−0.006 (3)
C10	0.048 (4)	0.050 (4)	0.044 (3)	−0.004 (3)	0.001 (3)	−0.008 (3)
C11	0.072 (5)	0.063 (4)	0.046 (4)	−0.004 (4)	−0.005 (4)	−0.002 (3)
C12	0.081 (6)	0.078 (5)	0.058 (4)	−0.021 (5)	0.014 (5)	−0.003 (4)
C13	0.054 (4)	0.080 (5)	0.063 (4)	−0.023 (4)	0.012 (4)	−0.010 (4)
C14	0.046 (4)	0.065 (4)	0.047 (4)	−0.011 (4)	0.005 (3)	−0.007 (3)

Geometric parameters (Å, º)

Br1—C5	1.901 (5)	C4—H4	0.9300
Cl1—C10	1.727 (6)	C5—C6	1.375 (10)
Cl2—C14	1.736 (8)	C6—H6	0.9300
O1—C2	1.349 (7)	C7—H7	0.9300
O1—H1O	0.827 (14)	C8—C9	1.466 (9)
N1—C7	1.276 (7)	C8—H8	0.9300
N1—N2	1.417 (7)	C9—C10	1.402 (9)
N2—C8	1.234 (7)	C9—C14	1.400 (8)
C1—C6	1.393 (8)	C10—C11	1.388 (9)
C1—C2	1.411 (9)	C11—C12	1.375 (10)
C1—C7	1.448 (8)	C11—H11	0.9300
C2—C3	1.382 (9)	C12—C13	1.384 (11)
C3—C4	1.384 (9)	C12—H12	0.9300
C3—H3	0.9300	C13—C14	1.392 (10)
C4—C5	1.369 (10)	C13—H13	0.9300
C2—O1—H1O	114 (6)	C1—C7—H7	118.5
C7—N1—N2	110.9 (5)	N2—C8—C9	124.5 (6)
C8—N2—N1	114.9 (5)	N2—C8—H8	117.8
C6—C1—C2	118.8 (5)	C9—C8—H8	117.8
C6—C1—C7	119.3 (5)	C10—C9—C14	116.1 (6)
C2—C1—C7	121.9 (5)	C10—C9—C8	125.3 (6)
O1—C2—C3	118.8 (6)	C14—C9—C8	118.6 (6)
O1—C2—C1	121.9 (6)	C11—C10—C9	121.5 (6)
C3—C2—C1	119.3 (5)	C11—C10—Cl1	116.2 (5)
C2—C3—C4	120.4 (6)	C9—C10—Cl1	122.3 (5)
C2—C3—H3	119.8	C12—C11—C10	120.6 (7)
C4—C3—H3	119.8	C12—C11—H11	119.7
C5—C4—C3	120.6 (6)	C10—C11—H11	119.7
C5—C4—H4	119.7	C11—C12—C13	120.0 (7)
C3—C4—H4	119.7	C11—C12—H12	120.0
C4—C5—C6	119.9 (5)	C13—C12—H12	120.0
C4—C5—Br1	120.4 (6)	C12—C13—C14	118.9 (7)
C6—C5—Br1	119.7 (6)	C12—C13—H13	120.6
C5—C6—C1	120.9 (6)	C14—C13—H13	120.6
C5—C6—H6	119.5	C13—C14—C9	122.9 (6)
C1—C6—H6	119.5	C13—C14—Cl2	116.3 (6)

N1—C7—C1	123.1 (6)	C9—C14—Cl2	120.8 (5)
N1—C7—H7	118.5		
C7—N1—N2—C8	177.8 (6)	N1—N2—C8—C9	−179.2 (6)
C6—C1—C2—O1	179.3 (6)	N2—C8—C9—C10	−13.9 (10)
C7—C1—C2—O1	−0.2 (9)	N2—C8—C9—C14	164.6 (7)
C6—C1—C2—C3	−1.0 (8)	C14—C9—C10—C11	1.0 (9)
C7—C1—C2—C3	179.4 (5)	C8—C9—C10—C11	179.5 (6)
O1—C2—C3—C4	−179.7 (6)	C14—C9—C10—Cl1	−179.2 (5)
C1—C2—C3—C4	0.6 (9)	C8—C9—C10—Cl1	−0.6 (9)
C2—C3—C4—C5	0.5 (10)	C9—C10—C11—C12	−0.6 (10)
C3—C4—C5—C6	−1.1 (10)	Cl1—C10—C11—C12	179.5 (5)
C3—C4—C5—Br1	179.9 (5)	C10—C11—C12—C13	0.1 (10)
C4—C5—C6—C1	0.6 (9)	C11—C12—C13—C14	−0.1 (11)
Br1—C5—C6—C1	179.6 (4)	C12—C13—C14—C9	0.5 (11)
C2—C1—C6—C5	0.4 (8)	C12—C13—C14—Cl2	−178.5 (6)
C7—C1—C6—C5	180.0 (5)	C10—C9—C14—C13	−0.9 (10)
N2—N1—C7—C1	−178.9 (5)	C8—C9—C14—C13	−179.6 (6)
C6—C1—C7—N1	−179.3 (6)	C10—C9—C14—Cl2	178.0 (5)
C2—C1—C7—N1	0.3 (9)	C8—C9—C14—Cl2	−0.6 (9)

Hydrogen-bond geometry (Å, º)

D—H···*A*	*D*—H	H···*A*	*D*···*A*	*D*—H···*A*
O1—H1*O*···N1	0.83 (6)	1.96 (6)	2.655 (8)	141 (7)